PERGAMON

Chaos, Solitons and Fractals 16 (2003) 841–852

CHAOS
SOLITONS & FRACTALS

www.elsevier.com/locate/chaos

A robust, locally interpretable algorithm for Lyapunov exponents

Florian Grond [a,*], Hans H. Diebner [a], Sven Sahle [b], Adolf Mathias [a], Sebastian Fischer [c], Otto E. Rossler [c]

[a] *Center for Art and Media, Institute for Basic Research, Lorenzstr. 19, 76135 Karlsruhe, Germany*
[b] *European Media Laboratory, Villa Bosch, Schloß-Wolfsbrunnenweg 33, 69118 Heidelberg, Germany*
[c] *Division of Theoretical Chemistry, University of Tübingen, Auf der Morgenstelle 8, 72076 Tübingen, Germany*

Abstract

An enhanced version of the well known Wolf algorithm for the estimation of the Lyapunov characteristic exponents (LCEs) is proposed. It permits interpretation of the local behavior of non-linear flows. The new variant allows for reliable calculation of the non-uniformity-factors (NUFs). The NUFs can be interpreted as standard deviations of the LCEs. Since the latter can also be estimated by the Wolf algorithm, however, without local information on the flow, the new version ensures local interpretability and therefore allows the calculation of the NUFs. The local contributions to the LCEs which we call "local LCEs" can at least be calculated up to three dimensions. Application of the modified method to a hyperchaotic flow in four dimensions shows that an extension to many dimensions is possible and promises new insight into so far not fully understood high-dimensional non-linear systems.

1. Introduction

The most prominent feature of chaos is its sensitive dependence on the initial conditions which is measured by the so-called Lyapunov characteristic exponents (LCEs). These entities are invariant global indicators in non-linear systems which describe the development of small errors in non-linear flows [1]. Unfortunately, one usually has to rely in numerical estimates [2]. In this paper we discuss the problems of local interpretation. A variant of the frequently used Wolf algorithm is introduced which allows to gain the important advantage of information on the local behavior of the dynamics which in turn allows for a more reliable statistical analysis.

Recall the definition of the LCE [3]. For a continuous dynamical system described by an autonomous ordinary differential equation (ODE) the number of LCEs is equal to the number of dimensions. Assume a temporal discretization, $\triangle t$, of the flow then the LCEs can be defined as follows:

$$\lambda_i = \lim_{N\to\infty} \lim_{\triangle t\to 0} \frac{1}{N\triangle t} \ln[S_i(M_N)], \tag{1}$$

where

$$M_N = \prod_{i=0}^{N} \mathrm{e}^{J(i\triangle t)\triangle t}. \tag{2}$$

* Corresponding author.
E-mail address: grond@zkm.de (F. Grond).

0960-0779/03/$ - see front matter
PII: S0960-0779(02)00479-4

Here the S_i are the singular values of the matrix M_N, and J is the Jacobian. In the case of ODEs, N is the number of performed integration steps of length $\triangle t$. Note, that in the case of maps, the term $e^{J(i\triangle t)\triangle t}$ needs to be replaced by $J(i)$ and the symbol $\lim_{\triangle t\to 0}$ disappears.

The above definition of the Lyapunov exponents (Eqs. 1 and 2) cannot be directly converted into a practical algorithm because of the numerical problems due to the singular value decomposition $S_i(M_N)$. More precisely, the argument M_N of the singular value decomposition in Eq. 1 is a product of an, in the limit $N \to \infty$, infinite number of matrices (Eq. 2). This cannot be decomposed into a product of the singular value decomposition of the individual matrices $e^{J(i\triangle t)\triangle t}$ [2]. An intuitive interpretation would be a unit sphere which is transformed into an ellipsoid by the matrix product M_N. The singular values are then associated with the principal axes of that ellipsoid, i.e. with vectors. In the case of chaotic systems an iterated application of this phase space deformation would relatively quickly lead to an extremely stretched ellipsoid. In other words, this product inevitably leads to a bad conditioning number.

Although the global average mean cannot be obtained by a simple accumulation of diverging and contracting directions obtained from an analysis of the local phase space of all points on the attractor as Wolf himself pointed out [4], the problems are usually elegantly circumvented by the frequently used so-called Wolf algorithm [4]. This algorithm calculates the LCEs as long time averages of perturbations in linear subspaces along the numerically computed trajectory, but supplies no interpretable information about the local development of perturbations in chaotic flows. In addition, as we shall show in the paper in hand, the local contributions are even misleading if taken too seriously. Although, in the long run the local errors seem to cancel out on average. Departing from the Wolf algorithm we introduce a variant that leads to locally interpretable values. The main advantage of the new algorithm is the capability to calculate the non-uniformity-factor (NUF) for each LCE.

2. Brief description of the Wolf algorithm

As mentioned the basic idea of the Wolf algorithm is to keep track of perturbations away from the trajectory in linearized phase space. Linearization is necessary because in the full non-linear phase space exponential growth of small perturbations away from the trajectory cannot be expected in the long run for chaotic attractors. In addition, in linear phase space the development of perturbations away from the trajectory is always proportional to the size of the perturbation. Hence, the value of the perturbation can be chosen in a numerically suitable way. Confer Ref. [4] for a detailed discussion of the consequences of linearization.

The perturbations away from the trajectory are described by n orthogonal vectors living in the linearized phase space with the latter defined through the Jacobian of the flow. Since the Jacobian is not constant, the non-linear system has to be integrated simultaneously to continuously update the linearized vector field.

An important concomitant procedure in Wolf's algorithm is the necessary re-orthogonalization of the set of n vectors usually performed by the method of Gram–Schmid. Without re-orthogonalization the vectors would become collinear and were oriented along the direction of the largest divergence in phase space. To ensure the orientation of one vector along the direction of the largest divergence of the flow it is important to orthogonalize the vectors always in the same order so that the orientation of the first vector is never changed by the orthogonalization. In the next step the orthogonalization procedure removes this component from the remaining set of vectors leaving for the second vector only the possibility to evolve into the direction of the second largest divergence of the flow. The same consideration applies for the remaining vectors. When the algorithm has converged, that is, after the mean magnitudes of stretching and contraction of all vectors do not change any longer, one finds the largest LCE as the mean length of the first vector and the others in descending order.

3. The local behavior in Wolfs algorithm and the new variant

In order to motivate the modification we re-examine Wolf's algorithm. To demonstrate the functioning of the Wolf algorithm we apply it to the Lorenz system looking at a periodic solution in a first step. The three perturbation vectors are orthogonalized after each integration step. The resulting local orientations of the three vectors describe three strips along the trajectory in their time course. This is depicted in Fig. 1. As proved by Haken the tangential direction contributes to the zero-exponent [2]. Therefore, the outcome of the Wolf algorithm confirms for the periodic solution the theoretical finding, although in an unexpected way without any fluctuations. In Fig. 1 one can make the interesting observation that the vector corresponding to the zero-exponent is permanently oriented in the tangential direction. One sees that the strips width indeed shrinks to zero and can therefore locally be distinguished from both remaining vectors belonging to the negative exponents (Confer LCE2, LCE3 in Fig. 1).

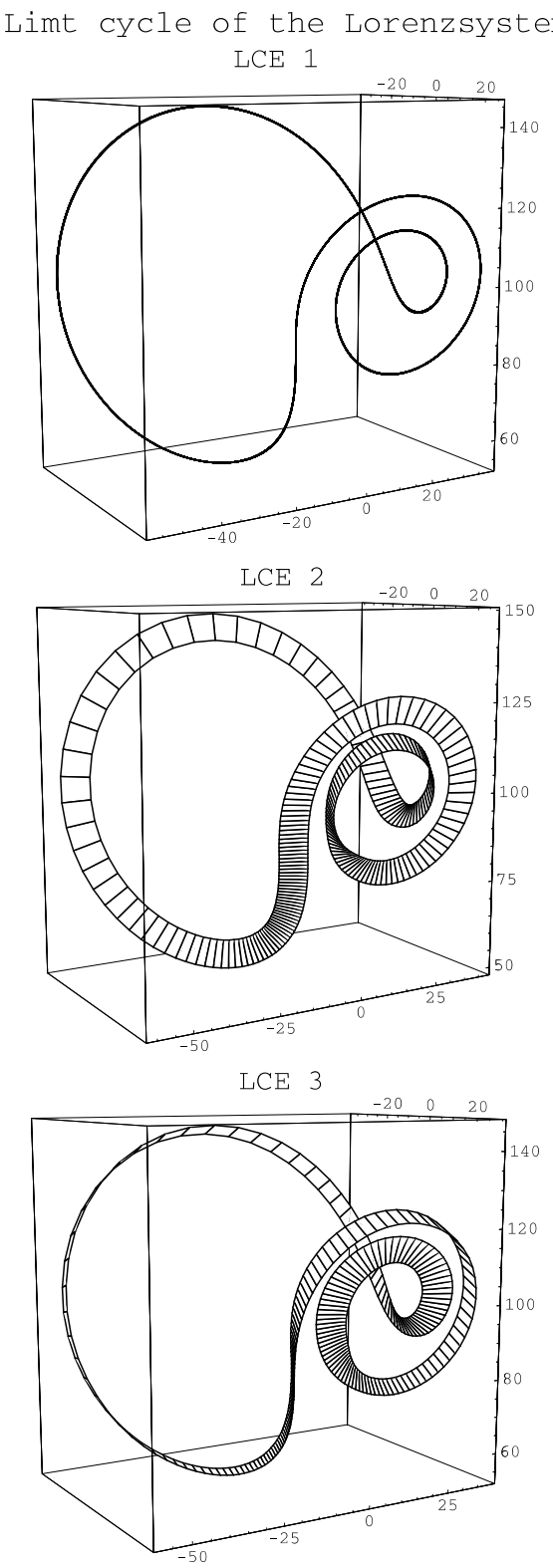

Fig. 1. Limit cycle solution of the Lorenz system showing a band structure corresponding to the local directions accumulating the global LCEs computed using the Wolf's algorithm. For details please confer text.

The situation for a chaotic solution looks different. In particular, the positive and the zero-exponents, the latter corresponding to the tangential direction, cannot be matched locally to vectors since they seem to exchange their orientations during the course of time (left column of Fig. 2). While the tangential direction is not always given by the

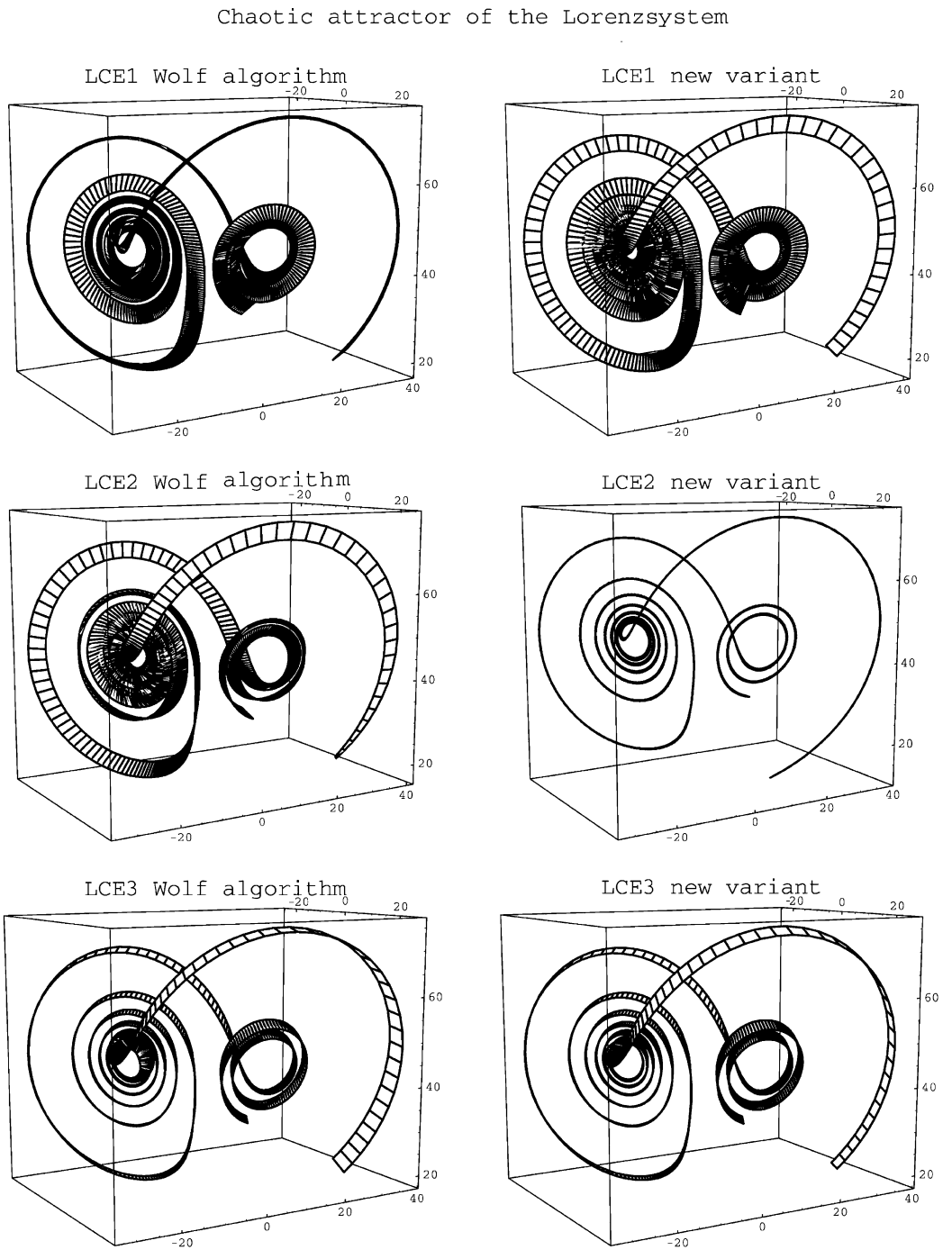

Fig. 2. Comparison of the local behavior of Wolf's algorithm and the new version in an application to a chaotic solution of the Lorenz system. The orientation of the strip corresponding to the local contributions to the negative exponent (LCE3) depicted in the lower two figures are identical, whereas the are pronounced differences of the band structures between the two versions for LCE1 and LCE2. Details are discussed in the text.

direction of the second largest divergence, nevertheless the latter corresponds to the zero-exponent in a chaotic case. It may however become momentarily the direction of the largest divergence. The re-orthogonalization procedure in Wolf's algorithm, however, forces the vector that describes the largest divergence in phase space to drift into the tangential direction. Indeed in the case of a chaotic solution the algorithm does not stabilize one vector into the tangential direction unlike what was seen in the periodic case above. Surprisingly, the Wolf algorithm nonetheless leads to reliable time average values of the LCEs in the long run. However, an interpretation in terms of the local structure of phase space is not possible.

Table 1
List of numerical results of both algorithms for periodic solutions of the Rossler system ($a = 0.2$, $b = 0.2$, $c = 8$), the Lorenz system ($\sigma = 10$, $R = 100.5$, $b = 8/3$) and a hyperchaotic system ($a = 0.6$, $b = 0.5$)

Periodic solutions	New variant	Wolf algorithm
Rossler		
LCE1	0.00582558	0.0120721
NUF1	1.72716	1.73977
Quantile (97.5%)	0.729829	1.07569
Quantile (2.5%)	−3.61791	−4.06937
LCE2	−0.0331616	−0.0132116
NUF2	1.50289	1.44134
Quantile (97.5%)	1.07727	0.951536
Quantile (2.5%)	−3.55018	−3.04878
LCE3	−7.25935	−7.27144
NUF3	5.51826	5.51730
Quantile (97.5%)	2.28465	2.41484
Quantile (2.5%)	−20.0043	−20.0067
Lorenz		
LCE1	−0.0012356	0.00148129
NUF1	7.60630	7.60787
Quantile (97.5%)	15.3614	15.3617
Quantile (2.5%)	−16.4649	−16.4639
LCE2	−1.78576	−1.78444
NUF2	7.89839	7.89845
Quantile (97.5%)	11.8538	11.8541
Quantile (2.5%)	−18.9084	−18.9094
LCE3	−11.7041	−11.7092
NUF3	10.7076	10.7090
Quantile (97.5%)	2.49183	2.49219
Quantile (2.5%)	−27.9346	−27.9347
Hyperchaos		
LCE1	0.00000129927	0.00000768202
NUF1	0.147039	0.147035
Quantile (97.5%)	0.218602	0.218509
Quantile (2.5%)	−0.292873	−0.292786
LCE2	−0.0618665	−0.0618729
NUF2	0.226663	0.226654
Quantile (97.5%)	0.345166	0.345166
Quantile (2.5%)	−0.473012	−0.472793
LCE3	−0.326601	−0.326890
NUF3	0.429619	0.430975
Quantile (97.5%)	0.425837	0.429579
Quantile (2.5%)	−1.17183	−1.16087
LCE4	−0.327984	−0.327696
NUF4	0.419687	0.420471
Quantile (97.5%)	0.401655	0.403379
Quantile (2.5%)	−1.13217	−1.13001

The table contains the global LCE (mean), the NUF as well as the 2.5% and 97.5% quantiles of the distribution of the local LCEs for each case.

In order to obtain an algorithm that gives also locally reliable results we propose to fix one vector into the tangential direction and associate it with the zero-exponent. We regard this to be an improvement since the genuine feature of chaos is the exponential growth of deviations orthogonal to the trajectory, although a momentary exponential growth of small errors into the tangential direction is possible, but a property of stable periodic solutions as well. The fixing of one vector along the tangential direction can easily be achieved by starting the re-orthonormalization procedure with the tangential vector, if this is followed by projecting the distorted vector set onto the orthogonal n-pode. The resulting algorithm leads to the same global values as the Wolf algorithm, although, in slightly changed order. The zero-exponent

Table 2
List of numerical results of both algorithms for chaotic solutions of the Rossler system ($a = 0.2$, $b = 0.2$, $c = 5.7$), the Lorenz system ($\sigma = 10$, $R = 45.92$, $b = 8/3$) and a hyperchaotic system ($a = 0.6$, $b = 0.05$)

Chaotic solutions	New variant	Wolf algorithm
Rossler		
LCE1	0.0731403	0.072771
NUF1	0.951882	0.992449
Quantile (97.5%)	2.07476	2.32671
Quantile (2.5%)	−2.16172	−2.52010
LCE2	0.000891036	0.0012604
NUF2	1.15874	1.08384
Quantile (97.5%)	2.29867	1.92839
Quantile (2.5%)	−3.83630	−3.49776
LCE3	−5.27427	−5.27427
NUF3	4.95080	4.95080
Quantile (97.5%)	2.85706	2.85706
Quantile (2.5%)	−14.0604	−14.0604
Lorenz		
LCE1	1.22859	1.19963
NUF1	2.76070	5.11451
Quantile (97.5%)	7.91185	11.2615
Quantile (2.5%)	−2.14720	−9.13656
LCE2	0.000209229	0.0000429642
NUF2	5.07274	2.37816
Quantile (97.5%)	10.1717	5.35315
Quantile (2.5%)	−9.14726	−3.60406
LCE3	−14.7574	−14.7283
NUF3	4.77321	4.77828
Quantile (97.5%)	−4.98052	−4.84506
Quantile (2.5%)	−22.8120	−22.7572
Hyperchaos		
LCE1	0.0901872	0.0939201
NUF1	0.587061	1.10506
Quantile (97.5%)	1.13083	2.86779
Quantile (2.5%)	−1.26627	−2.72599
LCE2	0.0220259	0.0243778
NUF2	0.624834	0.765998
Quantile (97.5%)	1.17714	1.87005
Quantile (2.5%)	−1.44237	−1.99173
LCE3	−0.00399829	−0.0019275
NUF3	1.37554	0.690455
Quantile (97.5%)	3.30801	1.29807
Quantile (2.5%)	−3.66361	−1.69498
LCE4	−1.28400	−1.28377
NUF4	2.45489	2.45576
Quantile (97.5%)	2.22899	2.22899
Quantile (2.5%)	−7.69895	−7.69895

The table contains the global LCE (mean), the NUF as well as the 2.5% and 97.5% quantiles of the distribution of the local LCEs for each case.

is fixed first and then come the remaining LCEs in descending order. This has been verified for several chaotic attractors. The results are compiled in Table 1 (periodic solutions) and Table 2 (chaotic solutions).

The local behavior of the modified algorithm is depicted in the left column of Fig. 2 for the same chaotic case as above. Comparing the new variant with the behavior of the Wolf algorithm (right column of Fig. 2) there is not only the expected effect of improved orientations for the zero and the positive exponent, but also is it remarkable that the orientation of the vector of the negative exponent is not affected by fixing the first vector in tangential direction. A plausible explanation of the latter observation would be the almost negligible thickness of the attractor leading to a approximately two-dimensional object. Any vector orthogonal to an arbitrary pair of vectors on this flat object has an orientation that is invariant under rotation of this pair of vectors. A similar result holds true for the hyperchaotic case discussed in the following section.

4. Results for a hyperchaotic equation

We now apply the improved algorithm to the following hyperchaotic equation [5] to demonstrate its functioning in a higher-dimensional case.

$$\begin{aligned} \dot{x} &= -y, \\ \dot{y} &= x - w, \\ \dot{z} &= -w + 0.3z, \\ \dot{w} &= a + 3w(y+z) - 2bw. \end{aligned} \tag{3}$$

Here again, first a limit cycle solution as well as the case of a hyperchaotic attractor are investigated. As in the three-dimensional case above both algorithms locally show comparable behaviors for the limit cycle situation. This is what one can observe looking at the time series of the local scalar stretchings and contractions depicted in Fig. 3.

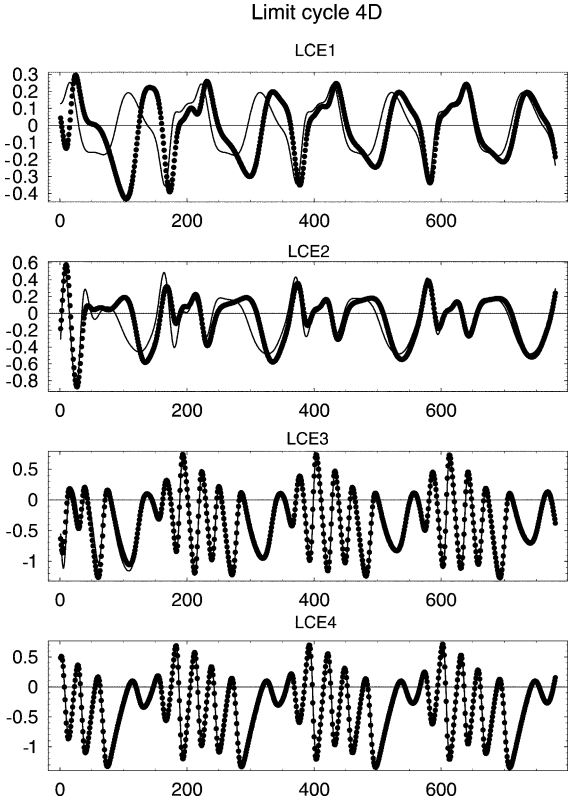

Fig. 3. Time series of the four local LCEs defined in Section 3 for a limit cycle solution of a four-dimensional non-linear system for both algorithms. The bold dotted curves belong to Wolf's algorithm, the thin line to the new version. The time scale is given in equidistant steps of re-orthogonalization.

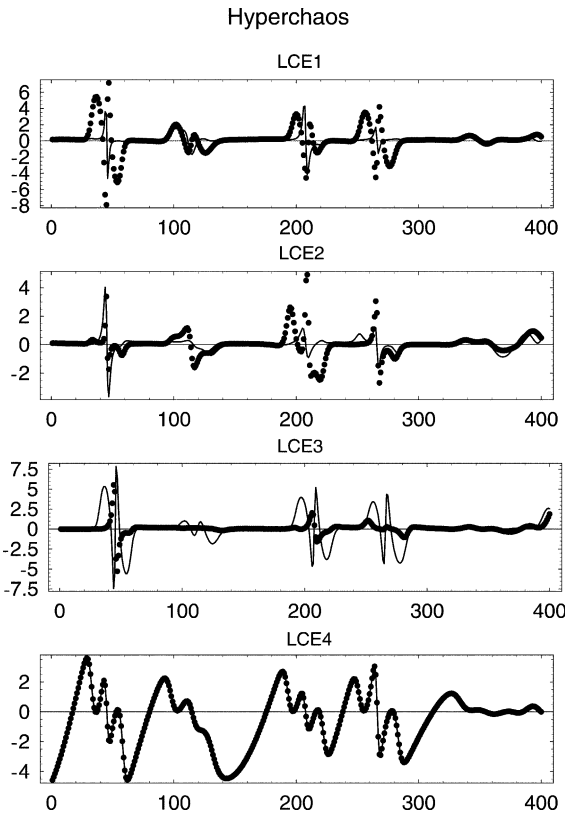

Fig. 4. Time series of the four local LCEs defined in Section 3 for a hyperchaotic solution of a four-dimensional non-linear system for both algorithms. The bold dotted curves belong to Wolf's algorithm, the thin line to the new version. The time scale is given in equidistant steps of re-orthogonalization. Note the similarity of the time series of LCE1 (dotted line) computed with Wolf's algorithm and LCE3 (thin line) computed with the new version. Details are discussed in the text. Compare with the distributions of the local exponents depicted in Fig. 5.

Interestingly the Wolf algorithm has a transient phase after which its results adjust to those of the modified algorithm. In the Wolf algorithm both LCE1 and LCE2 which correspond to the two locally least stable directions of attraction, need considerably more time to approach the behavior of the new algorithm.

Fig. 4 shows the temporal behavior of the local exponents for the hyperchaotic case. Here the results are again different for both algorithms, except for LCE4, as also observed in the three-dimensional case above (Fig. 2). The difference becomes even more marked if one regards the four distributions of the local LCEs (Fig. 5). Especially, when comparing the third distribution of the left column of figures and the uppermost distribution of the right column, one can see from the almost identical shapes of the distributions that the largest positive exponent of Wolf's method (right column) is paradoxically most of the time oriented along the tangential direction. This confirms the finding already obtained from the time series of Fig. 4. In the present figure the frequency, i.e. the y-axis, has a logarithmic scale in order to account for the sharp pulse-like shape of the distributions. The vertical lines represent the means (middle), the standard deviations are the pairs of lines enclosing the middle, the 2.5% and the 97.5% quantiles are the outermost pair, respectively. As already seen in the case of the Lorenz system (Fig. 2) the local values of the single negative exponent prove invariant under the modification of the algorithm.

5. The non-uniformity-factor

The NUF has been introduced by J. Nicolis for unimodal maps (cf. [3]) and can be identified with the standard deviation of the distribution of the local LCEs, denoted as γ_n. This factor reflects the fact that two dynamical systems

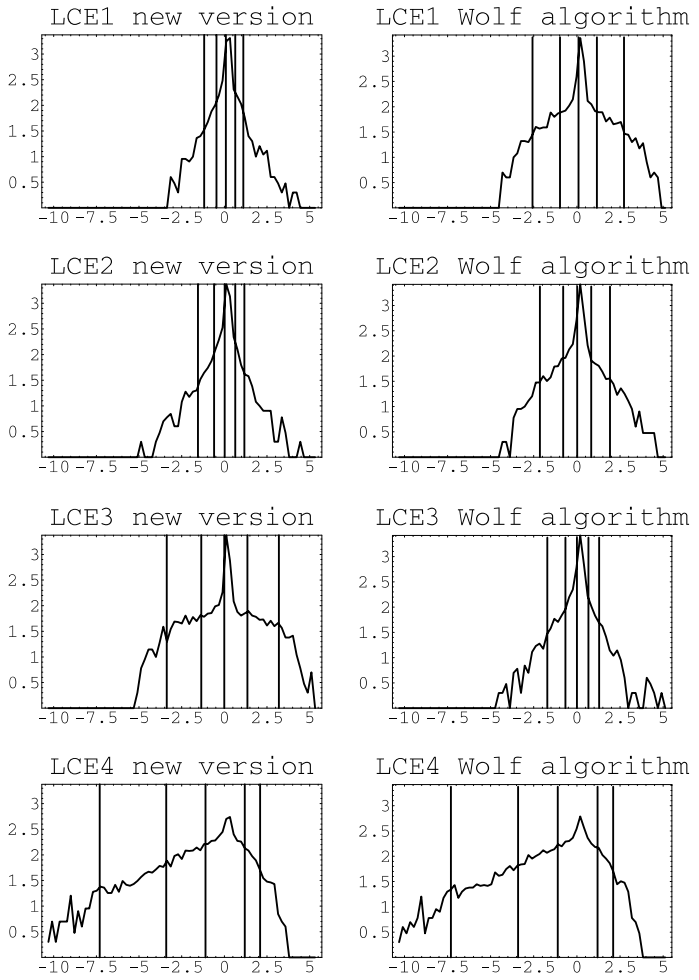

Fig. 5. Distributions of the local LCEs, computed by Wolf's algorithm (right column of figures) as well as with the new version (left stack of figures) corresponding to the same hyperchaotic case as in Fig. 4. Note, that the frequency, i.e. the y-axis, has a logarithmic scale to account for the sharp pulse-like shape of the distributions. The five additional vertical lines in each figure represent the means (middle), the standard deviations (pair of lines about the middle), the 2.5% and the 97.5% quantiles (the outermost pair), respectively.

with the same LCEs can locally show completely different dynamical behaviors corresponding to their different distributions of local LCEs. Of particular interest is the comparison of the tent map with the logistic map. The tent map produces chaos as a uniform stretching whereas in the logistic map periods of stretching alternate with periods of contraction. Nonetheless, both dynamical systems have the same LCEs (if the value of the growth parameter in the logistic map has been chosen to be 4 [6]). Therefore, the NUF provides relevant information about the local behavior of chaotic systems.

To derive the NUF for a unimodal map, recall the definition of the LCE:

$$\lambda = \lim_{N\to\infty} \frac{1}{N} \sum_{n=0}^{N-1} \ln \gamma_n, \tag{4}$$

where

$$\gamma_n = \left| \frac{\mathrm{d}F(x_n)}{\mathrm{d}x_n} \right| \tag{5}$$

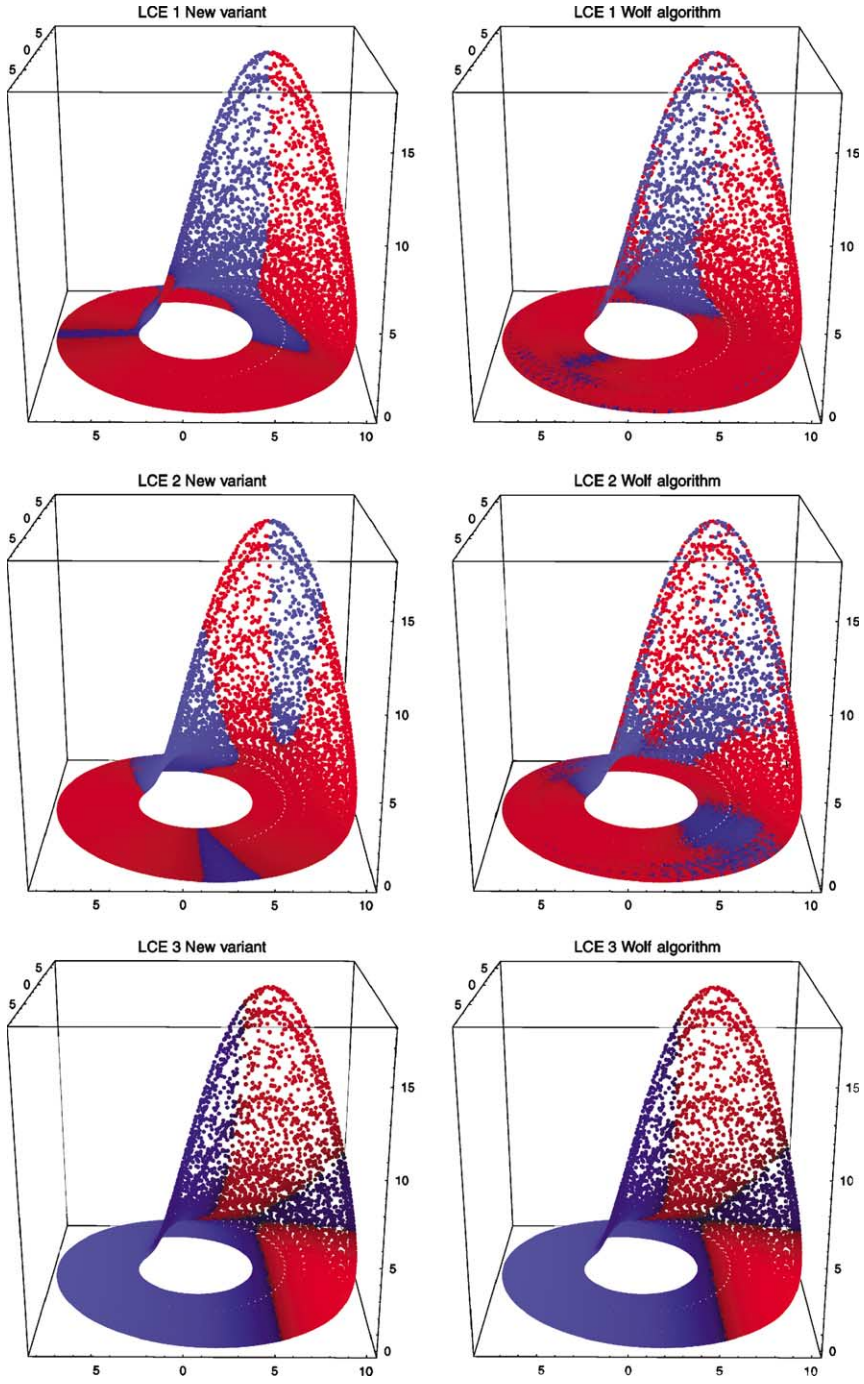

Fig. 6. Comparison of the behavior of the two algorithms in an application to the Rossler system. The local strength of contraction or divergence is color coded so that the contracting phases appear blue whereas the diverging phases appear red. Confer Section 6 for further discussion.

which then leads to the definition of the NUF as follows:

$$\mathrm{NUF} = \lim_{N\to\infty} \sqrt{\frac{1}{N}\sum_{n=0}^{N-1}(\lambda - \ln \gamma_n)^2}. \tag{6}$$

For the tent map, the NUF turns out to be 0, and for the logistic map, $\pi/\sqrt{12}$. Unfortunately, for higher-dimensional dynamical systems (maps as well as ODEs), there exists no similar analytical approach to quantify the local exponential growth or decay at a particular point on the attractor. Additionally, it cannot be decided to which LCE a local direction of stretching or contraction contributes. It was therefore of interest to analyze the local behavior of the Wolf algorithm in order to gain more knowledge on how the local values lead to the correct global mean.

The proper local orientation revealed by the new algorithm now allows one to use the distribution of the local LCEs to improve the knowledge of the local phase space structure which would otherwise only be reflected by the mean LCEs. This led us to apply the calculation of NUFs for the LCEs of multi-dimensional continuous flows, a concept that was introduced originally for unimodal maps only. The quality of the improved algorithm concerning the correct local orientations of the diverging, non-diverging and contracting directions, respectively, is illustrated through Fig. 6 for the Rossler attractor. Each of the three possible directions temporarily show contracting as well as diverging behavior. Contracting phases are coded blue whereas the diverging phases are red-coded. Clearly, the contracting direction are expected to exhibit much more frequently contracting phases than the diverging directions. Comparing the output for the new algorithm (left column) with the output of Wolf's algorithm (right column) one sees more fuzzy distributions in the latter case which we explain in the subsequent section.

6. Some further observations

The effects of the modified Wolf algorithm introduced so far is investigated in more detail in this section. Although a more rigorous mathematical investigation waits to be done—if possible at all—the following heuristic arguments seem to be convincing. The results obtained with the Rossler system have representative character and are scrutinized. In Fig. 6, it is interesting to observe that the improved algorithm is capable of detecting reliably the small contracting areas in the x–y plane of the Rossler attractor visualized as blue strips. These areas exist because the oscillations in the x–y plane differ from those of a harmonic oscillator, a fact, which leads to an elliptical distortion. The latter in turn results in an alternating contraction and expansion of the tangential direction and the one orthogonal to it, respectively. Therefore, the observation confirms what one would expect anyway for the local stability of a trajectory lying in that part of the Rossler attractor with approximately linear behavior. The Wolf algorithm blurrs these regions of local stability uncomprehensively over a broader range, as a consequence of the destabilized tangential direction in the chaotic case.

7. Discussion

One can clearly find the phenomena of the local behavior as shown in all figures perfectly reflected in the numerically obtained numbers. For example the similarity of the results of both algorithms (LCE, NUF, quantile 97.5%, quantile 2.5%) for periodic solutions (Table 1) and the deviations of the NUFs and quantiles for the positive and the zero-exponents in the chaotic case (Table 2). Since the computation of the LCEs have no analytical reference value, it is difficult to draw any conclusions about their accuracy. Neither it is appropriate to use the NUFs as an accuracy measure since they are just the calculations of the local contributions that are controversely debated. In Wolf's paper the figures are given with three significant digits only. Since the numerical zero-exponent has an analytical basis [2] it thus is the only value the numerical estimation of which can be assessed. This exponent can be estimated with strongly fluctuating quality from system to system. Hence we suggest the absolute value of the mandatory zero-exponent to be the order of magnitude the accuracy of the estimation of LCEs for a given dynamical system valid for either method be it the Wolf algorithm or the new variant. Since the theoretical result of the zero-exponent, which can be undoubtedly identified in the new method is exactly zero due to a sum with mutually cancelling terms the actual finite result can be attributed to numerical errors only. Even for the new algorithm, in which the tangential direction is fixed the numerical estimates are not better than those of the Wolf algorithm. This may be due to the perturbation in tangential direction that are evolved in the linearized phase space and later projected back onto the tangential vector. The projection may lead to undesired numerical artefacts, particularly in stiff equations as in the Rossler chaos. This proceeding remained from the Wolf algorithm and may be even avoided. The zero-exponent can be estimated in a more convenient way by calculating the logarithms of ratios of subsequent absolute values of the vectors emerging in each integration step. This issue will be discussed in detail in a forthcoming paper.

Using the new algorithm it was possible to reliably calculate the NUFs of the LCEs for continuous flows, since locally interpretable orientation of perturbations away from the trajectory, that accumulate the local LCEs is ensured. The effect of the adjustment of the local orientation, through fixing of the tangential direction, leads at least to the avoidance of blurring as seen and discussed in Fig. 6, but the effect can also be very pronounced as in the case of

hyperchaos (Figs. 4 and 5). The NUFs can be an interesting characteristic which may detect the onset of synchronization in coupled chaotic systems earlier than the time average of LCEs would.

This may lead to new insight for dynamical phenomenons in higher dimensions like hyperchaos or flare-attractors [7]. In these higher-dimensional dynamical systems there is the phenomenon of the so called Kaplan–Yorke chaos [1]. The conjecture of Kaplan–Yorke states, that a dynamical system with one positive LCE may make a unit-jump in dimensionality if the absolute value of one negative exponent is smaller than the positive one. Here the improved local understanding of the phase space and in particular the local contributions of stretching and folding to the more global means lend themselves for a better understanding of these phenomenons.

Furthermore a new possibility is on hand to compare LCEs obtained from data of time series with this new method. Usually the calculation of mostly the largest LCE from time series is achieved by the method of nearest neighbours [4,8,9]. In that method points situated in the near future of the trajectory (this is the tangential direction), are explicitly excluded from the set of used nearest neighbours. Using the new variant one has now the possibility not only to compare the global LCEs of time series computed from the model differential equation but also local contributions to the LCE of the time series with the reliable local reference values obtained through the new variant from the differential equation. By matching reconstructed attractors of time series to model differential equations it will be possible to asses the reconstruction process and the estimation of LCEs from time series by comparing not only the mean values but also the NUFs if a similar statistical measure were available for time series.

To conclude, a second generation version of the Wolf algorithm was proposed. Although its main features and usefulness were confirmed, it was possible to add a sort of standard deviation criterion by stabilizing the adherence of the algorithm to the local directions of stretching and contraction. Time will tell how much this improvement is worth in realistic scenarios.

Acknowledgements

We thank Kurt Bräuer, Klaus Sonnleitner, Wolf Koch, Axel Hoff, Günter Radons, and Jörg Becker for helpful discussions. We are also grateful to Anton Huber and Peter Weibel for their collaborations.

References

[1] Argyris J, Faust G, Haase M. Die Erforschung des Chaos. Braunschweig: Vieweg Verlag; 1994.
[2] Parker TS, Chua LO. Practical numerical algorithms for chaotic systems. NewYork: Springer Verlag; 1989.
[3] Leven RW, Koch BP, Pompe B. Chaos in dissipativen systemen. Berlin: AkademieVerlag GmbH; 1994.
[4] Wolf A, Swift JB, Swinney H, Vastano JA. Determining Lyapunov exponents from a time series. Physika D 1985;16:285–317.
[5] Baier G, Sahle S. Design of hyperchaotic flows. Phys Rev E 1995;51:2712–4.
[6] Grossman S, Thomae S. Invariant distributions and stationary correlations of the one dimensional logistic process. Z Naturforsch A 1977;32:1353–7.
[7] Hartmann GC, Rossler OE. Flaring-a new type of dynamical behaviour. In: Novak MN, editor. Fractal Review in the Natural and Applied Sciences. London: Chapmann & Hall; 1995.
[8] Parlitz U. Nonlinear time series analysis. In: Suykens JAK, Vandewalle J, editors. Nonlinear Modeling. Kluwer Academic Publishers; 1998. p. 209–39.
[9] Barna G, Tsuda I. A new method for computing Lyapunov exponents. Phys Lett A 1993;175:421–7.